

Keywords: nonlinear systems; electromagnetic vibrator; mathematical simulations; frequency response

Merab CHELIDZE^{1*}, Victor ZVIADAURI², Tamaz NATRIASHVILI³

SOME PROBLEMS WITH THE MATHEMATICAL MODELING OF ELECTROMAGNETIC VIBRATORS USED FOR TRANSPORTING BULK MATERIALS

Summary. Mathematical modeling with the original approach is used to study the dynamics of low-frequency electro-vibration machines while taking the technological load into account. Based on the mathematical analysis of differential equations describing the oscillatory motion of electromagnetic vibration exciters, the existing mathematical model has been corrected to describe the action of a semiconductor diode in the power circuits of single-cycle vibrators. Modeling nonlinear dynamic systems reveals the difficulties of obtaining the amplitude-frequency characteristics of the associated discrete change in the frequency of the driving force, as well as ways to overcome them.

1. INTRODUCTION

Vibrators are widely used in industry to produce mechanical vibrations. With the help of vibration technology, the compaction of concrete and other mixtures, the vibro transportation of loose (bulk) and viscous substances and the activation of chemical processes in liquid and loose media are effectively carried out. Among resonant vibrators, electromagnetic vibrators are widely used since electrical energy is simply supplied to them, and they effectively convert electrical energy into mechanical vibrations.

Electromagnetic vibration exciters can have different designs, but the basic principle of their operation is the same—that is, due to the pulsating electromagnetic field, a pulsation (oscillation) of two masses occurs, one of which is tied to the active mass (working body), while the other is tied to the reactive mass of the vibration exciter. Most often, electromagnetic vibrators are used as vibration exciters in transport machines to move and feed bulk materials, bunkers, stoves, furnaces, and feeders (Fig. 1a, whose electromagnet power supply diagram is shown in Fig. 1b) and in small installations to form reinforced concrete products.

It should be noted that the positive properties of electromagnetic vibrators are the absence of rubbing and rotating parts, which provides them with greater reliability and durability. In addition, they allow the smooth control of the amplitude of oscillations of the working bodies for various pieces of equipment. Both of these circumstances make electromagnetic vibrators indispensable in automated production lines of continuous operation. However, electromagnetic vibrators are significantly superior to electromechanical systems in terms of mass and size.

¹ R. Dvali Institute of Machine Mechanics; Mindeli 10, 0186 Tbilisi, Georgia; e-mail: m.chelidze47@gmail.com; orcid.org/0000-0001-8246-7533

² R. Dvali Institute of Machine Mechanics; Mindeli 10, 0186 Tbilisi, Georgia; e-mail: v_zviadauri@yahoo.com; orcid.org/0000-0001-7299-5770

³ R. Dvali Institute of Machine Mechanics; Mindeli 10, 0186 Tbilisi, Georgia; e-mail: t_natriashvili@yahoo.com; [orcid/0000-0001-9141-3641](https://orcid.org/0000-0001-9141-3641)

* *Corresponding author.* E-mail: m.chelidze47@gmail.com

Although electromagnetic vibrators have a very simple design, their theory and mathematical description of their dynamic and stability conditions are quite complex and include fundamental questions about the theory of vibration. When designing vibratory machines, the type of exciting force, the type of elastic systems, and their damping coefficients are of great importance since they play a major role in their dynamic stability during operation.

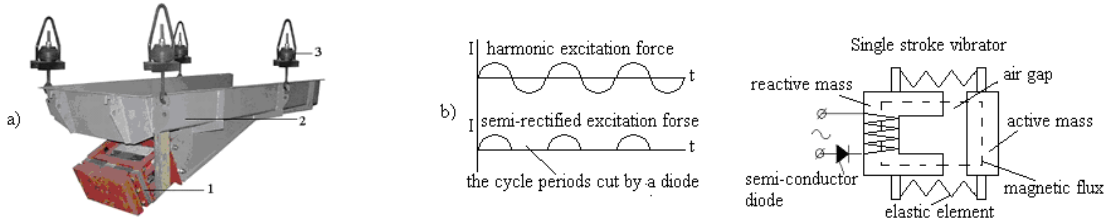


Fig. 1. A vibrating feeder with an electromagnetic vibrator: 1 - an electromagnetic vibrator; 2 - tray; 3 - pendants

2. ELECTROMAGNETIC EXCITER FORCE

The oscillations of the noted electromagnetic vibrators are described by the following differential equation [1 - 3]:

$$\ddot{x} + 2h\dot{x} + \omega_0^2 x = a\Phi^2 \tag{1}$$

$$\dot{\Phi} = b \sin(\omega t) - c(\delta - x)\Phi \tag{2}$$

where x is the amplitude of oscillations; ω is the natural circular frequency of the system; Φ is magnetic flux; δ is the air gap; a , b , and c are proportionality coefficients; and $2h$ is the coefficient of inelastic resistance according to the viscous model. This equation is equitable until the withdrawal of the air gap. After the impact of electromagnets, the oscillatory mode goes into vibro-shock mode.

Regimes of low-frequency oscillations are needed to realize the majority of technological operations. In an industrial network with a frequency of 50 Hz, the simplest and cheapest way to achieve a 50-Hz oscillation mode is to connect a semiconductor diode to the excitation coil circuit. In the numerical simulation, performed on the basis of scientific papers describing the mathematical modeling of single-cycle electromagnetic exciters excited by a semi-periodic force, unstable resonant modes arise. The real processes are shown in Fig. 2, and incorrect ones are in Fig. 3.

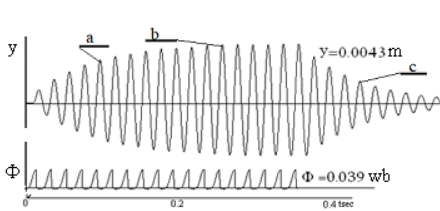


Fig. 2. y -amplitudes of the vibrator oscillation in meters, Φ -density of the exciting magnetic flux in Webers

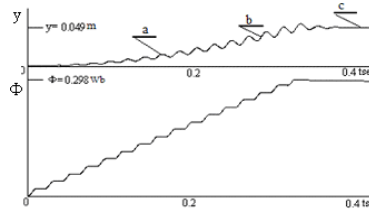


Fig. 3. Modes of resonance a-entry, b-stable, and c-exit from resonance under the condition of zeroing voltage

A number of works on modeling the balance of electric circuits described by differential equation (2) proposed that the semi-periodic rectification of alternating current and, therefore, magnetic flux into negative half-periods is equivalent to zeroing the member $\sin(\omega t)$ in equation (3).

$$b \sin(\omega t) = 0 \quad \text{when } \sin(\omega t) < 0 \tag{3}$$

This approach gives the solution shown in Fig. 3. To solve this problem, the electromagnetic vibrator excitation equation (3) was analyzed analytically, and according to the results obtained, certain adjustments were made to use it in the modeling process. To solve equation (3) analytically, it is assumed that the amplitudes of mechanical vibrations x in equation (1) are so low (or absolutely absent) that, with great accuracy, x may be omitted from equation (2).

In the given case, the analytical solution of equation (2) may be presented as the product of the functions $\Phi = u(t) \cdot v(t)$ [4, 5] when one of them is arbitrary and the other is defined based on equation (2).

$$\Phi = b \frac{c\delta \sin \omega t - \omega \cos \omega t}{(c\delta)^2 + \omega^2} + C^* e^{-c\delta t} \quad (4)$$

Under the initial conditions ($t=0, \Phi=0$), coefficient C^* is calculated as follows:

$$C^* = \frac{b\omega}{(c\delta)^2 + \omega^2} \quad (5)$$

After inserting Equation (5), Equation (4) is used to obtain the flow of magnetic flux [6]:

$$\Phi = \frac{b\omega}{(c\delta)^2 + \omega^2} e^{-c\delta t} + b \frac{c\delta \sin \omega t - \omega \cos \omega t}{(c\delta)^2 + \omega^2} \quad (6)$$

Equation (6) shows that the constant component of magnetic flux is changed according to the exponential law. With that, owing to the presence of the gap δ , the form of oscillations of magnetic flux is distorted slightly in comparison with the sinusoidal form.

In half-periodic rectification the member $b \cdot \sin \omega t$ in equation (2) works only in positive half-periods; in negative half-periods, the member $b \cdot \sin \omega t$ becomes zero, and equation (2) takes the following form:

$$\dot{\Phi} = -c\delta \Phi \quad (7)$$

where

$$\Phi = C^{**} e^{-c\delta t} \quad (8)$$

Under the initial conditions ($t=0, \Phi=\Phi_0$) the analytical solution takes the form of

$$\Phi = \Phi_0 e^{-c\delta t} \quad (9)$$

It is easy to see that an exponential decrease in Φ occurs over a very long period and in no way reflects the real disappearance of the magnetic flux. Naturally, at $t = 0.01$ s, which corresponds to a half-period of 50 Hz, Φ will not disappear to zero. Indeed, if magnetic flow is $\Phi = \Phi_0 = 1$ for $t=0$, then Φ become $\Phi = 0.99005$ for $t=0.01$. As a result, after n cycles, according to equation (2), a massive amount of false magnetic flux energy Φ accumulates, which is not explained in any way from the point of view of electrical engineering [6, 7, 8]. The inadmissibility of the substitution of equation (2) by equation (9) is also seen by considering the balance of supply circuit voltage:

$$ir = u \cdot \sin \omega t + W \dot{\Phi} \quad (10)$$

where u - is the amplitude of voltage, r denotes active resistance, and W is the number of coil windings.

In accordance with equation (10), in the absence of voltage u , the current i and its alteration, magnetic flux Φ , and the inductive resistance $W d\Phi/dt$ (Ldi/dt) of the electric circuit cannot exist [5,9]. The lack of member $u \cdot \sin \omega t$ in equation (10) leads to equation (11):

$$\dot{\Phi} = \frac{ri}{W} \quad (11)$$

In Equation (11), at the moment of absence of voltage $u \cdot \sin \omega t$ during the period when Φ disappears, the circuit can exist only in current i . Otherwise, Equation (10) loses its ability to describe the electromagnetic circuit.

It must be noted that equation (2) can be replaced by an equation (shown in [2]) describing electromagnetic force, which does not change the calculation.

There must be taken into account that when inductors or capacitors are in an AC circuit, the current and voltage do not peak at the same time. The small period difference between the peaks expressed in degrees (i.e., the phase difference between them $\varphi \leq 90^\circ$), is shown in fig.4. In the inductive circuits, the current lags the voltage in the positive phase. The phase is negative for a capacitive circuit since the current leads

the voltage. Electromagnetic waves carry energy through empty space, storing themselves in propagating electric and magnetic fields, wherein the change in the magnetic field is perpendicular to the electric field (Fig. 5) [9].

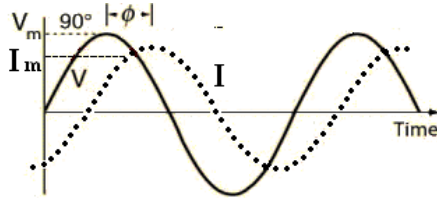


Fig. 4. The phase difference between voltage and current

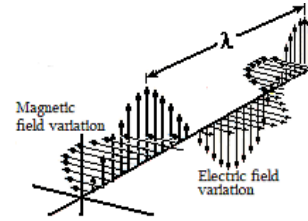


Fig. 5. Change in magnetic flux in accordance with the electric field

Therefore, according to Equation (2), in the negative half-periods of the alternating current $\sin\omega t$, it is necessary to make a replacement by a theoretical or experimental expression of the attenuation of the magnetic flux while maintaining the initial conditions for the equations [2,5]. The calculation in equation (2) can be simplified by equating Φ to zero at an insignificant assumption of error equivalent to the action of the semiconductor diode at the negative voltage [5].

$$\text{when } \sin(\omega t) < 0 \text{ then } \Phi = 0 \quad (12)$$

Taking into account the above corrections (12), we obtain the oscillatory process of an electromagnetic vibration exciter, which is in good agreement with the results of experimental studies on real electromagnetic vibration exciters (Fig. 6).

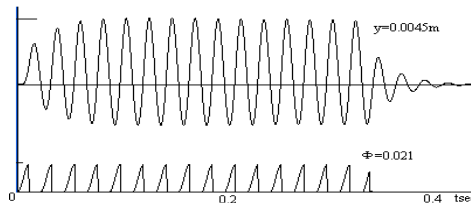


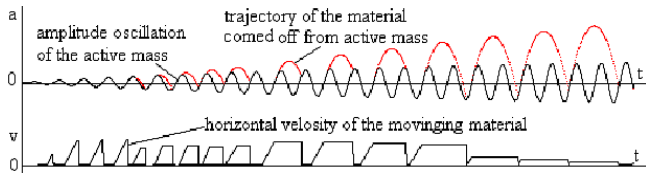
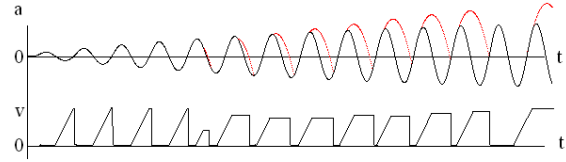
Fig. 6. y -amplitude of oscillations of the input, steady state and exit from the resonance mode, and Φ amplitude of the rectified magnetic flux

When describing the action of a semiconductor diode in a mathematical model, it should be kept in mind that a semiconductor diode does not cut off the so-called negative peaks of an alternating voltage; rather, it cuts off negative AC peaks. In turn, the peaks of the alternating magnetic flux circulating in the ferromagnetic circuit correspond in phase to the mechanical oscillations of the vibrator (Fig. 5). The phase shift between magnetic flux and the displacement amplitude is 180° and is absent with acceleration amplitude. It should be noted that the nonlinearities of the forces of stiffness, damping, and disturbance cause additional phase shifts between the given parameters [3,8].

Fig. 7 shows the trajectories of the amplitudes of the vertical movement of the working body of the vibrator (1) and the transported grain (2), as well as the horizontal speed (3) of the transported grain at excitation frequencies of 50 Hz (Fig. 7a) and 25 Hz (Fig. 7b).

Oscillograms of this type were obtained for the first time using a mathematical model that is in the process of development. This mathematical model will allow us to study the dynamic processes of a two-mass system under conditions of a variable technological load while taking into account nonlinear excitation and damping. Vibratory machines are two-mass systems, but they are considered single-mass systems to simplify the calculations.

The determination of the amplitude-frequency characteristics (AFC) of nonlinear resonant vibration machines is one of the main issues to consider when determining the dynamic characteristics and stability during operation. As a rule, knowledge of such characteristics is important for nonlinear resonant systems.

Fig. 7a. At the amplitude $a=0.05$ mm., $v=15$ mm/cFig. 7b. At the amplitude $a=1.5$ mm., $v=30$ mm/c

3. NONLINEAR SYSTEMS' FREQUENCY RESPONSES

With the harmonic excitation of a linear mechanical system (13), the obtained frequency response has the following form (Fig. 8):

$$\ddot{x} + 2h\dot{x} + \omega_0^2 x = a \sin \omega t \quad (13)$$

Theoretically, in the nonlinear systems with hard characteristics (14), if the forcing frequency ω changes very slowly (quasistatically) and discontinuously (with interruptions) from a low frequency (1) to a high frequency (3), a sequence of steady states will be obtained. When the point marked 3 is eventually reached, the system response jumps to the lower branch point (4), as indicated by the downward arrow in Fig. 9 [10].

$$\ddot{x} + 2h\dot{x} + \omega_0^2(x + cx^3) = a \sin \omega t \quad (14)$$

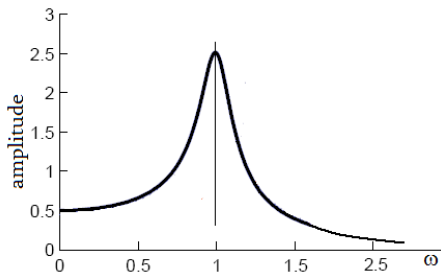


Fig. 8. AFC of a linear system

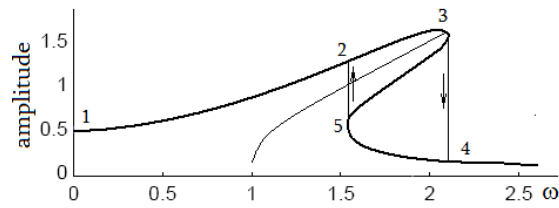


Fig. 9. AFC of a nonlinear system

Finally, as the forcing frequency decreases, the system response stays on the lower branch and, after crossing the point marked 5, jumps to point 2. Between these jumps, theoretically, there are three possible solutions, of which 2-3 and 4-5 are real stable realizable solutions and 3-5 is not realized; that is, the intermediate is unstable. When the system is started under arbitrary initial conditions, then which response the system chooses (upper or lower) depends on initial conditions [10].

Unfortunately, when digitally modeling nonlinear systems—for example, when using Runge-Kutta (i.e., with a discrete increase or decrease in the excitation frequency)—the possibility of obtaining an AFC that completely reflects the nonlinear dynamic property of the machine practically does not succeed (especially at low damping ratios of $\phi < 0.1$) [11]. In nonlinear systems, many oscillation cycles are required to establish stable amplitudes, and at low damping coefficients, a small step of the disturbance frequency change ($h < 0.1$) is required. However, there is no guarantee that these amplitudes will not move to a lower branch. During discrete switching from one excitation frequency to another, an imbalance of phases occurs between the electromagnetic excitation and potential (or kinetic) forces of the vibrator, making the mode of mechanical vibrations unstable [2, 11, 12].

With a discrete change in the excitation frequency in a nonlinear system, a process of a sharp increase or decrease in the amplitudes of stationary oscillations occurs. That is, in an oscillatory system with rigid characteristics (14), a discrete change of the excitation frequency causes a shift in the peak of the resonance curve towards higher frequencies. A sharp increase or decrease in the transient amplitudes of the oscillatory

process causes the amplitudes to jump towards the lower stable branch (i.e., small vibration amplitudes are established) (Fig. 10).

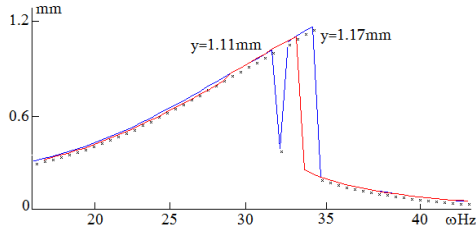


Fig. 10. AFC of a hard nonlinear system obtained by digital modeling without current time correction. $A=5555$, $2h=15$

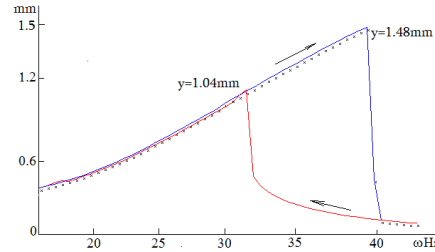


Fig. 11. AFC of a hard nonlinear system obtained by digital modeling with current time correction. $a=5555$, $2h=15$

At the moment when the discrete frequency is switched to maintain the phase between the forces, the current time step must be adjusted so that $\varphi_1 = \omega_1 t$ changes to $\varphi_2 = \omega_2 \tau$, where t is the current time step and τ is the corrected time step and is used only in moment of transition to a new frequency. Then, the process continues in step time t , with φ_1 representing the current discrete argument, ω_1 representing the current angular frequency, and φ_2 representing the new discrete argument corresponding to the new angular frequency ω_2 . In other words, at the moment of transition to a new frequency, instead of t , one should use the corrected time step τ equal to $\tau = \omega_1 t / \omega_2$ [2]. Such a correction creates a stable transient oscillatory process (even with a transition step of $2 \div 3$ Hz.), leading to the AFM characteristic of nonlinear systems shown in Fig. 11.

Figs. 12 and 13 show AFC obtained when taking into account uncorrected (Fig. 10) and corrected here (Fig. 11) (i.e., taking into account the phase shift between the perturbation forces and the oscillations of the mechanical amplitudes).

The lower AFC (curves) in Figs. 12 and 13 clearly show a decrease in the perturbation force (coefficient a) (i.e., a decrease in the magnitude of the oscillating amplitudes) decreases the effect of nonlinearity. At small amplitudes of oscillations (coefficient $a=1555$), the corrected and uncorrected (unadjusted) frequency characteristics become the same. It should be noted that in the mathematical modeling of nonlinear systems, it was necessary to use a double floating point number; otherwise, in most cases, the influence of nonlinearities would be lost since, when measuring in the SI system, we would have had to deal with values that were too small—for instance, $y=(0.001\text{m})^3=0.000000001\text{m}^3=10^{-9}\text{m}^3$.

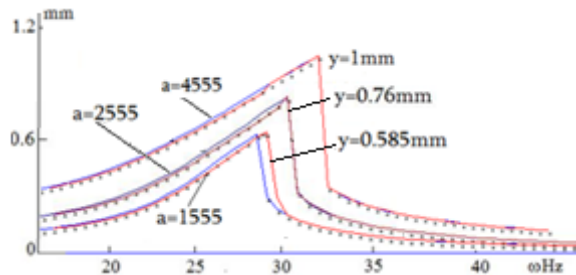


Fig. 12. AFC of hard nonlinear systems obtained by digital modeling without current time correction. $2h=15$

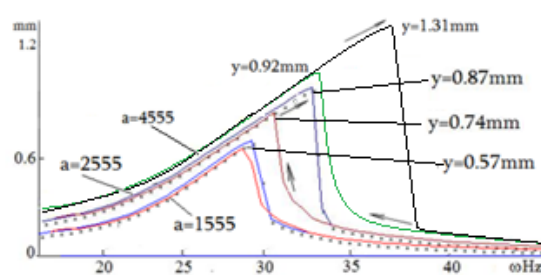


Fig. 13. AFC of hard nonlinear systems obtained by digital modeling with current time correction. $2h=15$

Fig. 14 and Fig. 15 show the frequency response (AFC) of a nonlinear system when the coefficient of resistance is $2h = 5$ (i.e., when the damping coefficient is below $\phi < 0.1$). As shown in Fig. 13, in this case (when $\phi < 0.1$ and in the uncorrected current time), the time used to stabilize the amplitudes (10–15 cycles) is obviously small. At a certain time, a different number of vibrational cycles occurs at low and high frequencies. From Fig. 13, it is seen that when correcting the current time, the amplitudes are stabilized and there is no sharp change in the amplitudes of the oscillations.

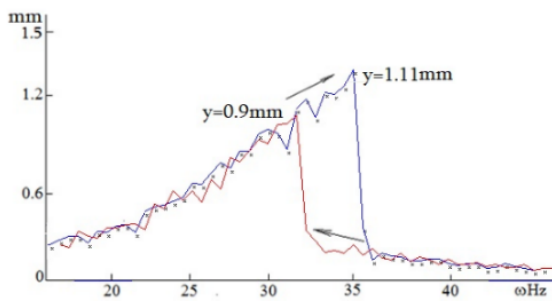


Fig. 14. AFC of a hard nonlinear system without current time correction. $2h=5$, $a=2555$

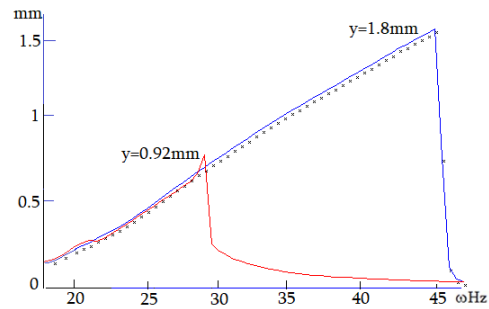


Fig. 15. AFC of a hard nonlinear system with current time correction. $2h=5$, $a=2555$

Fig. 16 shows the frequency response when large dissipative forces act in the system, which can be associated with internal scattering (damping coefficient) and process load. In this case, the obtained frequency characteristics of both corrected and uncorrected current time coincide. Large resistance forces stabilize the amplitudes of oscillations and drastically reduce the time needed for the transition process.

Fig. 17 shows the frequency response (AFC) for a nonlinear system with a soft characteristic in accordance with Equation (15).

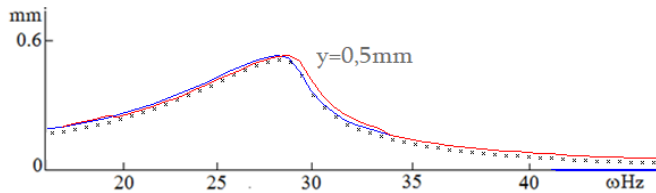


Fig. 16. AFC of a hard nonlinear system without and with current time correction. $2h=30$, $a=2555$

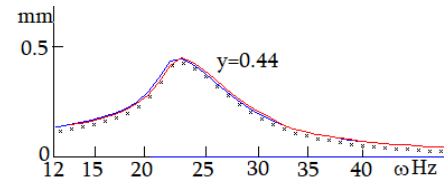


Fig. 17. AFC of a soft nonlinear system without and with current time correction. $2h=50$, $a=3555$

An analysis of the obtained frequency response shows that more powerful dissipative and disturbing forces are required to generate stable amplitudes of the same magnitude as those for nonlinear systems with a rigid characteristic.

$$\ddot{x} + 2h\dot{x} + \omega_0^2(x - cx^3) = a \cdot \sin \omega t \quad (15)$$

This is due to the fact that a decrease in the resonance frequency causes the peak of the resonance frequency to shift to lower frequencies. Therefore, the fraction of acquired and dissipated energy increases due to an increase in the cycle time. This effect is especially prominent for electromagnetic vibrators because when the frequency decreases, the inductive resistance of the electromagnetic circuit decreases; therefore, the energy used by the vibrator increases [9].

Figs. 18 and 19 show the frequency responses of nonlinear systems with reduced dissipative and disturbing forces. In this case, the corrected current time makes it easy to obtain the frequency response, which is typical for nonlinear systems with a soft characteristic.

In some cases, the exciting frequency is nonlinear, especially for electromagnetic vibrators, in which case the harmonic excitation frequency is presented in the second power (Equation (1)) [2,5]. Mathematical research has shown that instead of two equations with sufficient accuracy, it is possible to replace two equations with one [2].

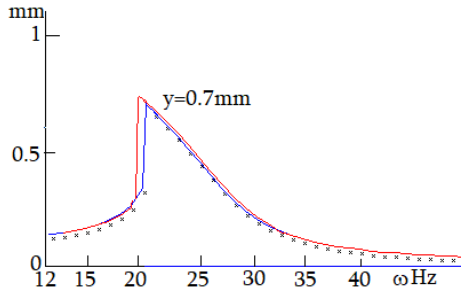


Fig. 18. Frequency response of a soft nonlinear system without current time correction. $2h=27$, $a=2555$

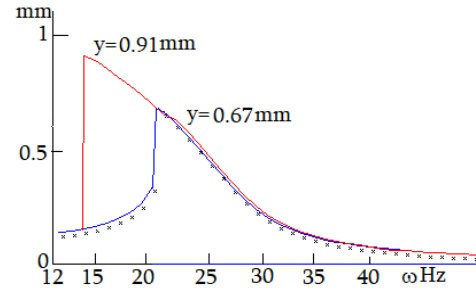


Fig. 19. Frequency response of a soft nonlinear system with current time correction. $2h=27$, $a=2555$

$$\ddot{x} + 2h\dot{x} + \omega_0^2(x + cx^3) = a(\sin\omega t)^2 \quad (16)$$

In this case, we present the solution of a nonlinear system with a rigid characteristic in which the perturbing force is presented as a quadratic degree without equation (2). In approximate calculations, it is very convenient to use this equation since the absence of equation (2), which describes the nonlinear electromagnetic force, simplifies the calculations and eliminates the danger of the unrealistic accumulation of disturbing energy in the oscillatory system.

The quadratic degree of harmonic disturbing force doubles the frequency of the disturbance. It is sometimes necessary to block (cut off) the positive or negative half-periods of the harmonic disturbing force to reduce the frequency of the disturbance.

Figs. 20 and 21 show the frequency responses obtained using equation (16) with a semi-periodic rectification of the perturbing harmonic force, taking into account the time correction (uncorrected and corrected time). A comparison of the obtained AFC with purely harmonic AFC. Fig. 11 shows that the oscillation amplitudes decrease since, in this case, the energy is supplied only for half of the cycle period.

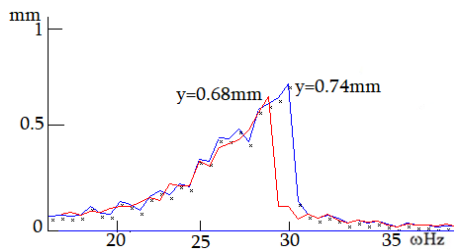


Fig. 20. AFC of a nonlinear system without current time correction. $2h=27$, $a=2555$

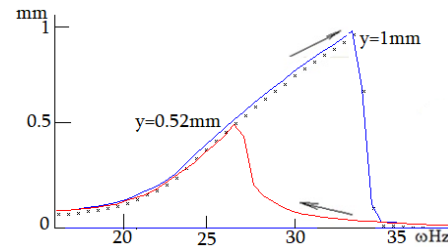


Fig. 21. AFC of a nonlinear system with current time correction. $2h=27$, $a=2555$

In this case, it is also necessary to use time control (current corrected time) to obtain a nonlinear frequency response for a nonlinear system.

Fig. 22 shows the frequency response in the presence of an increased damping coefficient. As in the previous cases, an increase in the damping coefficient and a small amplitude of oscillations minimize the influence of nonlinearity on the dynamics of the machine. Therefore, the obtained AFC using both corrected and uncorrected current times are the same.

Fig. 23 shows the frequency response (AFC) of the 50-Hz resonant mode with an increased damping coefficient. Therefore, the obtained corrected and uncorrected frequency responses are the same. The perturbing force was increased by almost three times when comparing the 25-Hz resonance regime with the 50-Hz regime. This is necessary because the elastic stiffness at 50 Hz exceeds the stiffness of the 25-Hz mode by four times.

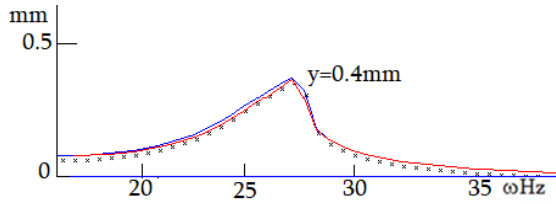


Fig. 22. AFC of a nonlinear system without and with current time correction. $2h=30$, $a=2555$

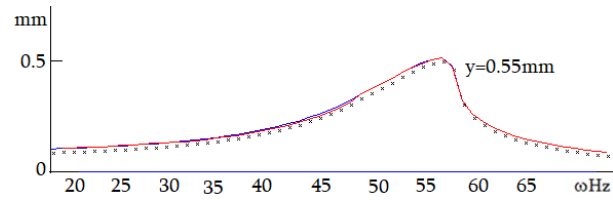


Fig. 23. AFC of a nonlinear system without and with current time correction. $2h=50$, $a=9555$

Figs. 24 and 25 show the frequency characteristics of uncorrected and corrected 50-Hz semi-periodic excitation of resonant modes with reduced resistance in the frequency range of 17–70 Hz. A multiple 25-Hz mode appears on both oscillograms. When modeling by purely harmonic force with the same parameters, the peak of the 25th frequency does not occur.

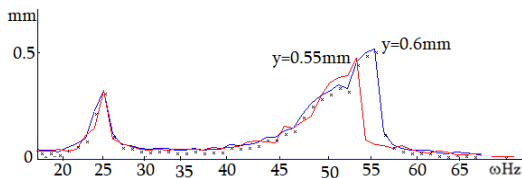


Fig. 24. AFC of a nonlinear system without current time correction. $\phi=5$, $a=5555$

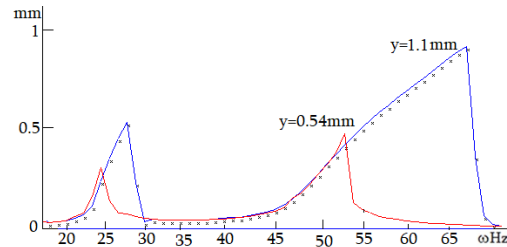


Fig. 25. AFC of nonlinear system with current time correction. $\phi=5$, $a=5555$

Fig. 26 shows the frequency response of a nonlinear resonant mode obtained when excited by a semi-rectified force in the frequency range of 7-61 Hz, taking into account the soft characteristic and using differential equation (15). In Fig. 27, a rigid characteristic is applied according to equation (16). Studies using numerical experiments have shown that multiple harmonics are formed as a result of the nonlinearity of the excitation force (in our case, as a result of the force of half-period excitation). The frequency response shows oscillograms of the mechanical oscillations of the displacement and acceleration amplitudes, which have an asymmetric and distorted sinusoidal shape.

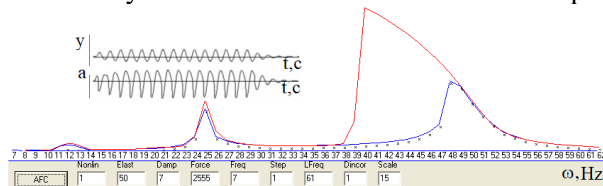


Fig. 26. 50-Hz AFC with cut-off half periods of exciting force

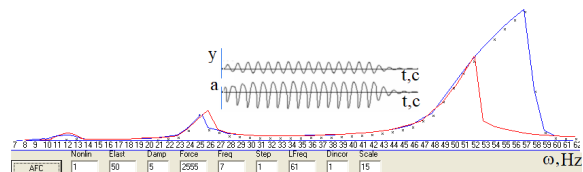


Fig. 27. 50-Hz AFC with cut-off half periods of exciting force

Fig. 28 shows the frequency response obtained with the harmonic excitation of the oscillatory system by linear stiffness at a frequency of 50 Hz. The oscillograms show the mechanical oscillations of displacement and the acceleration of the amplitude, which have symmetrical and sinusoidal forms. Fig. 29 shows the

frequency response obtained when excited by a semi-rectified current with the corresponding amplitudes of asymmetric displacements and accelerations, the sinusoidal shape of which is also additionally distorted. This asymmetry and distortion cause a number of harmonics to form, including a subharmonic resonance at 25 Hz.

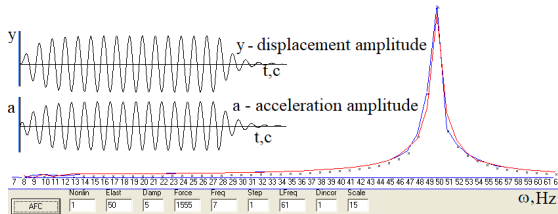


Fig. 28. AFC of a nonlinear system without current time correction. $\phi=5$, $a=5555$

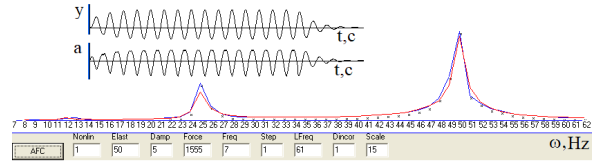


Fig. 29. AFC of a nonlinear system with current time correction. $\phi=5$, $a=5555$

Fig. 30 shows the frequency response with the corresponding oscillograms of the displacement and acceleration of mechanical oscillations caused by the action of a harmonic excitation force acting according to Equation (2). Due to frequency doubling during harmonic excitation (a semiconductor diode is not included in the electrical circuit), resonant oscillations do not occur at an excitation frequency of 50 Hz (left oscillogram). The resonant mode occurs at an excitation frequency of 25 Hz (right oscillogram). The acceleration amplitudes are sinusoidal and symmetrical, so multiple harmonics are not generated. Fig. 31 shows the oscillatory resonance mode of asymmetric displacement and acceleration amplitudes with the corresponding frequency responses of multiple resonances resulting from a half-rectified drive current.

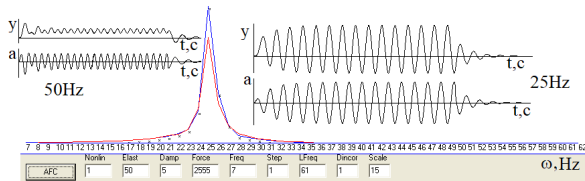


Fig. 30. AFC of a nonlinear system without current time correction. $\phi=5$, $a=5555$

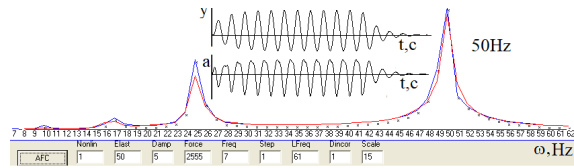


Fig. 31. AFC of a nonlinear system with current time correction. $\phi=5$, $a=5555$

Thus, the asymmetry and distortion of the sinusoidal shape of the acceleration amplitudes of a mechanical system generated by the action of nonlinear excitation cause the occurrence of multiple harmonics, including the subharmonic resonance mode, which, under certain conditions (at low dissipation forces), can seriously damage structures.

4. CONCLUSION

On the basis of theoretical analysis and experimental studies, some problems that arise in the mathematical modeling of single-cycle vibrators were solved. Simulation studies have proven that the electromagnetic excitation force leads to the nonlinearity of the electromagnetic vibrators, which is the reason for the generation of multiple harmonic resonances.

The above results obtained through mathematical experiments are in good agreement with the results obtained in real physical experiments.

In a defined frequency area of any nonlinear systems, two stable resonance regimes with high or low amplitudes of oscillations are generated. For high nonlinear amplitudes to be obtained by mathematical

simulation, it was necessary that at discrete changing driving frequency ω the correction of current time t was such that the shift φ was remained unchanged.

The mathematical model created for this study on nonlinear systems frequency response can be widely used in vibration technology applications.

According to the results of experimental and digital studies, it can be said that the developed mathematical model (simulator) can be used to determine the operational dynamic parameters of electromagnetic vibrators in the design process.

References

1. Blekhman, I.I. *Vibrational Mechanics: Nonlinear Dynamic Effects, General Approach, Applications*. World Scientific Publishing Company. 2000. 536 p. ISBN: 9810238908.
2. Крюков, Б.И. *Динамика вибрационных машин резонансного типа*. Киев: Наукова думка. 1967. 210 p. [In Russian: Krukov, B.I. *Dynamics of vibration machines of resonant type*. Kyiv: Naukova Dumka].
3. Zviadauri, V. & Chelidze, M. & Tedoshvili, M. *Dynamics of Vibratory Technological and Processes of Movement of the Friable Materials on the Spatially Vibrator in Plane*. LAMBERT Academic Publishing. 2021. 147 p.
4. Chelidze, M. & Zviadauri, V. Generating of sub harmonic resonant oscillations and problems of their stability. *JVE Journal of vibroengineering*. 2008. Vol. 10. No. 4. P. 483-486.
5. Piskunov, N. *Differential and Integral Calculus*. Vol. II MIR. Publications Moscow. Translated from Russian by George Yankovsky. 2021.
6. Purcells, E.M. & Morin, D.J. *Electricity and Magnetism*. Cambridge University Press. 2013. 839 p.
7. Moliton, A. *Basic electromagnetism and materials*. Springer-Verlag New York, LLC. New York City. 2007. 430 p. ISBN: 978-0-387-30284-3.
8. Despotović, Ž.V. & Jović, M. Mathematical model of electromagnetic vibratory exciter with incremental motion. *INFOTEH-JAHORINA*. 2014. Vol. 13. P. 91-96.
9. Moliton, A. *Basic electromagnetism and materials*. Springer-Verlag New York, LLC. New York City. 2007. 430 p. ISBN: 978-0-387-30284-3.
10. Zviadauri, V. & Tumanishvili, G. & Tsotskhalashvili, M. Mathematical model of complex control of the vibratory transportation and technological process. *Journal of Vibroengineering*. 2020. Vol. 22. No. 8. P. 1770-1781. DOI: 10.21595/jve.2020.20793.

Received 17.06.2021; accepted in revised form 28.11.2022